Published in final edited form as:
Dev Biol. 2014 September 1; 393(1): 71–83. doi:10.1016/j.ydbio.2014.06.019.

Transcriptional inhibition of *etv2* expression is essential for embryonic cardiac development

Marcus-Oliver Schupp[1], **Matthew Waas**[1], **Chang-Zoon Chun**[1,2], and **Ramani Ramchandran**[1]

Ramani Ramchandran: rramchan@mcw.edu

[1]Medical College of Wisconsin, Department of Pediatrics, CRI Developmental Vascular Biology Program, Translational and Biomedical Research Center, CRI C3420, 8701 Watertown Plank Road, P.O. Box 26509, Milwaukee, WI 53226, USA, Phone: 414-955-2387, Fax: 414-955-6325

[2]Division of Nephrology, Hypertension and Renal Transplantation, Room CG-98, 1600 Archer Road, University of Florida, Gainesville, FL 32610

Abstract

E-twenty six variant 2 (Etv2) transcription factor participates in cardiac, vascular-endothelial and blood cell lineage specification decisions during embryonic development. Previous studies have identified genomic elements in the *etv2* locus responsible for vascular endothelial cell specification. Using transgenic analysis in zebrafish, we report here an *etv2* proximal promoter fragment that prevents transgene misexpression in myocardial progenitor cells. This inhibition of *etv2* expression in the cardiac progenitor population is partly mediated by Scl and Nkx2.5, likely through direct binding to the *etv2* promoter, and cis-regulatory elements located in the first and second introns. The results identify an *etv2* cis-regulatory mechanism controlling cardiovascular fate choice implying that *etv2* participates in a transcriptional network mediating developmental plasticity of endothelial progenitor cells during embryonic development.

Keywords

zebrafish; transcription; cardiac disc; Etv2; Scl

Introduction

During vertebrate embryonic development, cells of the cardiac, blood and vascular lineages are specified from lateral plate mesoderm (LPM) via integration of inductive signals and systematic activation and deactivation of transcriptional programs in progenitor cells. Cardiac development in particular is orchestrated by a unique set of transcription factors that

Correspondence to: Ramani Ramchandran, rramchan@mcw.edu.

The authors declare that they have no competing financial interests.

All authors discussed the results, commented on the manuscript, and declared that no conflict of interest exists.

include Gata5, Hand2 and Nkx2.5. Stem cell like (Scl) and E26 transformation-specific domain (Ets) variant 2 (Etv2) factors have recently been added to this list. Specifically, *scl* represses cardiomyogenesis in prospective hemogenic endothelium and endocardium (Van Handel et al., 2012), and *etv2* function is necessary for repression of cardiac fate in putative endothelial-fated precursor cells (Palencia-Desai et al., 2011) suggesting the existence of a common progenitor cell of cardiac, blood and vascular lineages. Further support to this concept comes from a report showing a genetic link between hemangioblast and cardiac development (Peterkin et al., 2009). Endothelial, cardiac and blood precursor cells all arise in the anterior LPM shortly after gastrulation, and over the course of development, specification into each lineage occurs as distinct sets of transcription factors are silenced or activated. Factors Scl and Lmo2 are involved in hemangioblast development from anterior LPM (Patterson et al., 2007), and Hand2 and Nkx2.5 transcription factors (Thattaliyath et al., 2002) are essential for cardiac cell specification from LPM cell pools. *Nkx2.5* and *nkx2.7* genes play an essential role in maintaining ventricular and atrial cardiomyocyte identity (Targoff et al., 2013), and in establishing gene expression borders between cardiac cell lineages during heart development (Nakashima et al., 2014). Similar to Nkx2.5, Etv2 has also been recently implicated in cardiomyocyte development (Palencia-Desai et al., 2011). Because Etv2 appears to function at the interface of hematopoietic, vascular and cardiac lineage specification, we hypothesized that examination of *etv2* gene regulation will reveal mechanisms involved in the differentiation of sub-populations of blood, endothelial and cardiac cells from anterior LPM in zebrafish. Two studies (Proulx et al., 2010; Veldman and Lin, 2012) have already identified genomic fragments that control tissue-specific *etv2* expression during zebrafish embryonic development. Proulx et al. reported elements in the *etv2* genomic locus responsible for vascular-specific expression. Veldman et al. identified a 110 bp upstream enhancer of *etv2* that contains a functional binding site for Foxc1a and Foxc1b factors responsible for vascular-specific *etv2* expression. Here, by using transgenic reporter analysis of the *etv2* genomic locus, we identified cis-regulatory elements that are responsible for the transcriptional repression of the *etv2* gene in precursors of endocardial and myocardial cells. Using morpholino oligonucleotide-mediated knockdowns, we found that Scl and Nkx2.5 transcription factors participate in this repression mechanism. Cardiac inhibition of *etv2* expression is likely through sequence-specific binding of Scl to the *etv2* promoter as shown in a protein-DNA interaction assay. Moreover, using a dual-luciferase reporter system, we identified cis-regulatory elements located in the first two introns of *etv2*. Together, our studies reveal evidence for developmental plasticity of a progenitor cell of endothelial, endocardial and myocardial lineages that responds to *etv2* expression modulation during embryonic cardiovascular development.

Material and methods

Generation of transgenic zebrafish lines

Approximately 1 nL of each construct c1, c2 and c3 was microinjected into zebrafish zygotes at a final concentration of 25 ng/μL together with 25 ng/μL in vitro-transcribed transposase mRNA from NotI-linearized pCS2FA-transposase plasmid in 0.1% phenol red using a gas-driven microinjector (World Precision Instruments PV 820). See Supplemental Experimental Procedures for analysis of transgenic lines (Table S1). All animal experiments

were performed in accordance with guidelines and protocols (AUA 320) approved by the Institutional Animal Care and Use Committee at the Medical College of Wisconsin.

Whole-mount *in situ* hybridization (ISH)

Chromogenic detection of endogenous and transgenic transcripts (regular ISH) was conducted as described previously (Thisse and Thisse, 2008). Two-color fluorescent in-situ-hybridization (FISH) was performed with modifications described in the Supplemental Experimental Procedures section.

Imaging

Confocal z-stacks of stained specimen were acquired using an LSM 510 confocal microscope system (Zeiss). 3D images were reconstructed, processed and analyzed with Volocity 6.0.1 software (Perkin Elmer). Quantification of colocalization was performed using raw z-stack data in Volocity. M_{red} and M_{green} values correspond to colocalization coefficients M1 and M2 in a region of interest (ROI), with M1 describing the percentage of all red pixels colocalizing with green pixels, and M2 the percentage of all green pixels colocalizing with red pixels in an ROI (Zinchuk et al., 2007). R is the overlap coefficient according to previous studies (Manders et al., 1993). Background corrected ROIs (schematically indicated by blue dashed circles in Fig. S4) resulted in thresholded scatter plots ensuring reliability of colocalization and overlap coefficient calculations in Volocity.

Morpholino antisense oligonucleotides

Previously published and efficacy validated morpholinos for knockdown of *nkx2.5* (Goldstein and Fishman, 1998), *gata5* (Holtzinger and Evans, 2007), *hand2* (Trinh et al., 2005), *scl* (Gering et al., 1998) and *etv2* (Sumanas and Lin, 2006) were purchased from GeneTools, LLC, Philomath, OR, USA, and reconstituted in water to 2 mM stock concentration. Approximately 1 nL of injection mix containing 0.1% phenol red was microinjected into zebrafish zygotes. Sequences and doses used are given in the Supplemental Experimental Procedures section.

Luciferase assays

Fragments for cloning of zebrafish etv2- and myl7-based reporter constructs were PCR-amplified from p5E-3114 (see above) and BAC clone Ch211-87L2 (BACPAC Resources Center, Oakland, CA, USA), respectively. To amplify ampicillin/kanamycin coding sequence serving as replacements for *etv2* downstream sequence, TOPO-cloning vector pCR2.1 (Life Technologies) was used as template. Fragments with 15 bp overlapping sequence were PCR-amplified, and were cloned into the EcoRV-linearized pGL4.14 firefly Luciferase vector (Promega) using the In-Fusion cloning kit (Clontech) according to the manufacturer' s recommendations. Constructs were phenol-chloroform-extracted, ethanol-precipitated, sequence-verified, and used for zebrafish microinjections and H9C2 rat embryonic myocardium cell (ATCC, no. CRL-1446) transfections. For microinjections, respective firefly constructs and Renilla luciferase control reporter vector pRL-TK (Promega) were mixed at 66 and 33 ng/μL final concentrations, respectively, containing 0.1% phenol red, and 100-150 pg total DNA were injected into zebrafish zygotes. Forty

embryos were dechorionated by pronase (Sigma P5147) treatment, deyolked (Link et al., 2006) and lysed in 100 μL passive lysis buffer (Promega) at 6 and 22 somite stages. For H9C2 cell transfections, 10,000 cells per well were seeded in 24-well plates and grown for 48 h at 37°C and 5% CO2 in complete medium composed of DMEM, 20% Hi-FBS and 1% penicillin/streptomycin (Life Technologies). Transfection mixes contained 40 μL serum-free medium, 5 μL H9C2 transfection reagent (Altogen Biosystems), 56 fmol Renilla control vector and 51 fmol respective firefly construct DNA in 49 μL total volume. Transfection mixes were incubated for 30 min at room temperature to allow for transfection complex assembly, then added to the cells in 500 μL fresh complete medium, and incubated for another 48 h. Luciferase expression measurements from both microinjections and cell transfections were executed in technical triplicates from three independent experiments using the Dual-Luciferase Reporter 1000 Assay System (Promega) in a GLOMAX 20/20 luminometer (Promega) according to the manufacturer's instructions.

Electromobility shift assay (EMSA)

Recombinant zebrafish Scl and Tcf3 (E12/E47) proteins were produced using the TNT™ T7 Quick for PCR DNA kit (Promega, Madison, WI, USA) according to the manufacturer's recommendations. Primer sequences for generation of template-DNA in TNT reactions, western blot and binding conditions are given in the Supplemental Experimental Procedures section.

Statistics

To assess the “goodness of fit” of distributions of (trans)gene expression magnitudes from categorized embryo numbers in morpholino knockdown experiments, exact 2-sided p-values were calculated using StatXact™ 8 software (Cytel Inc., Cambridge, MA, USA) applying Pearson's Chi-square and Fisher's Exact tests when needed. Statistical significance in luciferase assays was calculated using t-tests (two-tailed, unpaired) in Excel 2008 software (Microsoft) from three independent experiments with three technical replicates each. All error bars represent standard deviations. Statistically significant data with p-values ≤0.05 and ≤0.01 are marked in the figures by * and **, respectively. Statistically highly significant data (p ≤0.001) are marked by ***. The results section text includes calculated p-values.

Results

Etv2 genomic locus characterization

Our laboratory has previously identified that *etv2*+ cells at the lateral plate mesoderm (LPM) in zebrafish proliferate prior to migration to the midline during vasculogenesis (Chun et al., 2011). To investigate the transcriptional regulation of *etv2*, we performed bioinformatic analyses to identify genomic elements that direct the vascular specific expression of *etv2* during embryonic development. *Etv2 and fli1*, a second transcription factor with vascular function (Brown et al., 2000; Pham et al., 2007) are juxtaposed in opposite orientations on chromosome 16 with a space of approx. 4.1 kb distance between respective first exons separating the two genes (Figure S1A). Bioinformatic analysis showed two conserved regions in this interspersed genomic DNA, an upstream (-3.1 to -1.8 kb relative to TSS) and an intronic (+0.4 to +0.8 kb relative to TSS) region (*up1* and *int2* in Figure S1A). We

initially generated a series of constructs (Figure 1A) encompassing these two regions fused to fluorescent proteins (Kaede, mCherry or EGFP) in Tol2- or I-Sce I vector-based transgenesis systems. While our study was ongoing, a second independent study by Veldman et al (Veldman and Lin, 2012) published a putative 2.3 kb *etv2* promoter element. In that study, they narrowed down the 2.3 kb promoter to a conserved 110 bp region (*up1*) that was sufficient for vascular expression at 24 hpf. This region along with more upstream and another conserved intronic (*int2*) region described before (Veldman and Lin, 2012) were suggested to be responsible for driving robust *etv2* expression during development. Our analysis indicates that 5.1 kb, 4.1 kb, 3.2 kb and 3.1 kb *etv2* genomic fragments (Figure 1A, constructs c1, c5, c4 and c2, respectively), all containing both at least 2.17 kb upstream and downstream (encompassing exon 1 to intron 2) regions (Veldman and Lin, 2012) consistently showed vascular-endothelial expression. We performed ISH for the transgenes in these lines (Figure 1B). The 5.1 kb, 4.1 kb and 3.2 kb transgenic lines showed vascular expression of the reporter gene with minimal ectopic expression during late somitogenesis and early primordial stages (Figure 1B, constructs c1, c5 and c4). Surprisingly, robust vascular transgene expression pattern was also observed in transgenic lines generated from construct c6, which differed from constructs c1, c2, c4 and c5 by a truncated upstream region (0.6 kb, Figure 1A). This result, in contrast to results from the Veldman study (Veldman and Lin, 2012), indicated that most if not all distal promoter sequence is dispensable for vascular-specific expression of *etv2*. Constructs 2 (c2) and 3 (c3) both contain the same upstream region (-2.17 kb relative to TSS), but c3 lacks the downstream region encompassing exons 1 and 2 and introns 1 and 2 (Figure 1A). In the c2 transgenic lines (Figure 1B), we noticed that most aspects of vascular expression such as head, axial, and intersomitic vessels are present. Moreover, all transgenes harboring the downstream intronic region recapitulated the endocardial *etv2* expression domain (shown here for c2, marked by white arrows in Figure 1C). Strikingly, deleting downstream intronic sequence (c3) resulted in ectopic transgene expression in tissue surrounding the endocardial domain, which represents the myocardial domain of the embryonic heart (dotted circle in Figure 1C-c3). This pattern change was observed consistently in all independent transgenic lines generated from c3. Further, expression in the developing vasculature was reduced with few cells in the caudal plexus showing expression (Figure 1B, c3). Also, head and axial vessel expression was restricted compared to transgenic lines derived from constructs that contain downstream intronic sequence. Taking all these data together, we conclude that *etv2* promoter fragments comprising the downstream intronic region harbor the regulatory elements responsible for repressing myocardial expression, and maintaining endocardial and vascular expression of *etv2* during embryonic vascular development. Table S1 summarizes the expression patterns of the transgenes.

Transgene expressing cells in the downstream fragment-deleted c3 transgenic line change from endothelial/endocardial to myocardial expression patterns during somitogenesis

Since the majority of the Veldman et al. (Veldman and Lin, 2012) work focused on the up2 element, we have restricted our analysis here to the downstream intronic element (int2). The int2 element is highly conserved across fish species, and some homology to human sequence was detected as well (Figure S1B). To determine spatial differences in the co-expression of c2 (intron-containing) and c3 (intron-less) transgenes with vascular-endothelial and heart

markers, we focused on the anterior LPM expression at 6-8 som and on cardiac expression at 20-22 som (Figure 2), stages most relevant to cardiac precursor cell development in zebrafish (Schoenebeck et al., 2007). At 6-8 som, we performed comparative fluorescent ISH analysis of the c3 intron-less transgene with the endogenous *etv2* gene (Figure 2), as well as cardiac markers *nkx2.5*, *hand2* and *gata5* and blood marker *scl* (Figure S2). At 6-8 som, most if not all transgene expressing cells is *etv2*-positive (+) indicating a high level of recapitulation of the endogenous expression pattern by the c3 transgene (Figures 2A-C whereas in the c2). *Scl* also co-localized well with the c3 transgene at this stage (Figures S2A-C), while anterior *hand2*+ cells showed minimal if any c3 transgene activity (Figure S2D-F), and for *nkx2.5*, no overlap with transgene expression could be detected at the anterior LPM at 6-8 som (Figures S2G-I). Later at 20-22 som (Figure 2), in the c3 (intron-less) transgenic line, ectopic reporter expression in the cardiac disc showed no overlap with endogenous *etv2* expression (Figures 2D-F), whereas in the c2 (intron-containing) line, reporter expression maximally matched the *etv2* expression pattern (Figures 2G-I). The ectopic cardiac expression domain of c3 was identified as the myocardial precursor cell population co-expressing *nkx2.5* (Figure S2J-L) and *myosin light polypeptide 7* (*myl7*, formerly known as cardiac myosin light chain 2, Figure S2M-O). Interestingly, co-localization of the *c3* transgene with endogenous *etv2* in the cardiac disc (endocardial domain) appears minimal compared to the *c2* transgene (compare Figures 2F and 2I, white arrow indicates *etv2*+ endocardial cells in the center of the cardiac disc surrounded by myocardial, *nkx2.5*+ cells). In most cases, no signal for the *c3* transgene transcript was detected in the endocardial domain (e.g. Figures S2K, N, Q; see also Figure 1C-c3 and Figure 3A). Of note, we observed a general decrease in *c3* transgene expression over generations such as the signal in the anteriorly located head vessels became silenced in F5 embryos (Figure S2N) although still present in F2 embryos (Figure 2E and Figures S2K, Q). The transgene expressing cells co-localized with the *gata5*+ mesodermal (myocardial) expression domain (encircled in Figure S2P), whereas the flanking endodermal domains of *gata5* (stars in Figure S2P) were clearly negative for *c3* transgene expression (Figure S2R). In the c2 (intron-containing) transgenic line, however, transgene expression did not overlap with *gata5* in the myocardium (Figure S2S-U). In contrast, *c3* transgene expression was persistent in the zebrafish heart after 40 hpf (Figure S3A) and 64 hpf (Figure S3B). The transient presence of *c2* transgene mimics the endogenous *etv2* transcripts, which was hardly detectable after 36 hpf (Sumanas and Lin, 2006). This indicated a temporal misregulation of the *c3* transgene in addition to the observed spatial differences in its expression. Summarizing the ISH data at 6-8 and 20-22 som in the two transgenic lines (c2 & c3) suggests that during development, both transgenes are expressed for the most part in *etv2* expressing cells at early somitogenesis stages, but post the 8 som stage, the expression of the *c3* transgene localizes to myocardial progenitor cells. These data also suggest differential regulation of *etv2* expression in different cell types post early patterning events in the vertebrate embryo.

Changes in downstream fragment-deleted c3 transgene expression following knockdown of cardiac-specific transcription factors

Because putative *etv2* cis-regulatory sequence contains bioinformatically predicted binding sites for several heart-related transcription factors (Figure S1C), we knocked down each of

these factors, and performed ISH for the intron-less *c3* transgene to investigate changes in its expression level at 6-8 and 20-22 somite stages. We hypothesized that knocking down one or combinations of these factors would result in changes in transgene expression magnitude in the heart in the c3 transgenic line. Efficacy confirmed and validated morpholinos previously used in the zebrafish field (Patterson et al., 2005; Reichenbach et al., 2008; Sumanas and Lin, 2006; Targoff et al., 2008; Trinh et al., 2005) were microinjected into zygotes, and ISH was performed to reveal transgene expression at 6-8 som (Figure S3A & B), and 20-22 somite stages (Fig. 3). Independent transgenic c3 fish were mated with wild type fish to obtain quantifiable numbers of transgenic zygotes for injection. Different mating pairs generated embryos with varying transgene magnitudes most likely resulting from differences in transgene copy number genomic integration events. Following pooling and equal division of progeny of several mating pairs of independent c3 transgenic lines from different generations, we determined and counted the magnitude categories of transgene expression in embryos injected with either target-specific or non-targeting standard control morpholinos (MOs). The MOs were titrated to ensure that the reductions in respective gene expression levels did not result in morphologically obvious phenotypes such as absence of beating hearts in *nkx2.5* morphants or absence of circulating blood cells in *scl* and *etv2* morphants. Transgene expression magnitudes were categorized by visual assessment (very strong, strong, medium, weak, absent, or transgene negative). We scored numbers and show representative images of transgene expression categories at the respective embryonic stages (6-8 som and 20-22 som). Structure (anterior LPM, cardiac disc) and number of embryos (n) showing the respective category of transgene expression is provided in a color-coded percent format (number of embryos in each category divided by total number of embryos) for a given experiment.

At 6-8 som, loss-of-function (LOF) analysis using MOs that target *nkx2.5* (Figure S3B, p=0.22), *gata5* (Figure S3B, p=0.55), *scl* (Figure S3B, p=0.86), or *hand2* (Figure S3B, p=0.71) showed no significant changes in c3 transgene expression in the anterior LPM. At 20-22 som, we investigated transgene expression in the cardiac disc (marked by blue frame in Figure 3A) following knockdown of heart- and vascular-specific transcription factors. Compared to embryos injected with standard control MO, *nkx2.5* and *gata5* knockdowns resulted in polar opposite changes in *c3* transgene expression in that knockdown of *nkx2.5* lead to significantly greater number of morphants with strong transgene expression (Figure 3B1, strong, p=2.231e-006, n=93), and knockdown of *gata5* showed greater number of morphants with weak transgene expression (Figure 3B1, weak, p=0.0003, n=96) in the cardiac domain. In case of *scl* and *etv2*, single *scl* knockdown resulted in a greater number of morphants with strong transgene expression (Figure 3B2, p=0.007, n=109), and *etv2* morphants showed no relevant change (Figure 3B3, p=0.54, n=94). Knocking down *etv2* and *scl* together resulted in more morphants with strong c3 transgene expression in the cardiac disc (Figure 3B4, p=0.004, n=92) indicating that *scl* but not *etv2*-regulated c3 expression here. For *nkx2.5* and *etv2* double knockdown, we observed significant higher percentage of morphants with strong transgene expression in the cardiac domain (Figures 3B5 and S3A, p=2.047e-005, n=29), confirming that *nkx2.5* regulated the majority of c3 expression. Besides from increased cardiac *c3* expression, these morphants showed a concomitant increase in transgene expression in anterior head vessel progenitors (Figure S4B,

p=1.671e-012). In contrast, *c3* expression in more posteriorly located trunk vessel progenitors were not significantly changed (Figure S4C, p=0.602). This indicated that the de-regulated *c3* transgene was inhibited by *nkx2.5* in ALPM- but not PLPM-derived cardiac and endothelial progenitor populations, Since *nkx2.5* is not expressed by the EC lineage, this suggests a non-cell autonomous role for *nkx2.5* in of angioblast development. These data collectively suggest that *scl* and *nkx2.5* function together in repressing transgene expression in the cardiac disc in the c3 transgenic lines at 20-22 som, while *gata5* seems to antagonize the function of these genes.

Scl and *nkx2.5* function together to repress transgene expression in intron-less and intron-containing transgenic lines

To conclusively determine the roles of *scl* and *nkx2.5* in regulating transgene reporter activities, we knocked down *scl* and *nkx2.5* together in both c3 (Figure 3C and 3D) and c2 (Figure 3E-H) transgenic lines. In c3 intron-less lines, we observed the appearance of an additional category of “very strong” transgene expressing morphants (Figure 3C) and an increase in strong transgene expressing morphants compared to either transcription factor alone (Figure 3D, p=0.0002 and 0.001 compared to *nkx2.5* and *scl* single knockdowns, respectively), which was consistent with our earlier analysis, and indicated synergism of *scl* and *nkx2.5* in c3 transgene inhibition. In the c2 intron-containing line, we similarly observed that *scl* and *nkx2.5* double knockdown showed a more significant increase in the number of very strong (Figure 3G and H, p=5.677e-014, n=81) transgene expressing morphants compared to single *scl* knockdown (Figure 3E and F, p=1.043e-006, n=163). Interestingly, we noticed that *nkx2.5* knockdown alone showed significant increase in *c3* (Figure 3D, p=2.746e-007, n=176), but not c2 transgene expression (Figure 3F, p=0.58, n=128) when compared to control morphants, suggesting participation of *etv2* downstream sequence in *nkx2.5*-mediated inhibition of *c2* transgene expression.

Note that the distributions of reporter expression magnitudes in the control morphants differ across experiments because clutches from different independent transgenic lines per construct were pooled. This approach, combined with high embryo numbers per sample, maximized normalization of transgenic expression magnitudes across samples per experiment before injection and thus ensuring quantitation. To further ensure objective quantification of changes in transgene magnitudes in knockdown experiments, we performed two independent blinded embryo counts on wells containing single and combined *nkx2.5/scl* morphants at the 22 somite stage after MO injections and ISH detecting c3 transgene expression magnitudes (Fig. S5). According to the embryo numbers obtained for each category of cardiac transgene staining intensity, we were able to identify respective morphants based on previous results (Fig. 3). For example, embryos in well #3 were clearly identifiable as double *scl/nkx2.5* morphants. Therefore, the results and conclusions are affirmed in an objective test assessment.

We also performed two-color fluorescent ISH to investigate the spatial changes in *c2* and *c3* transgene expression in morphant cardiac discs following digital 3D reconstruction (Figure 4). In control morphants, cardiac expression of the intron-less *c3* transgene localized to both endocardial and myocardial domains and matched *myl7* expression maximally (Figure 4A-

C). In contrast, intron-containing *c2* transgene transcripts were present in the *myl7*- endocardial progenitor cell population (Figure 4M-O, medially located endocardial cells are marked by a dashed circle in Figure 4N). Upon knockdown of *scl*, increased endocardial expression of both *c3* (Figure 4D-F) and *c2* (Figure 4P-R) transgenes were observed indicating that de-repression of *etv2* expression caused an accumulation of endocardial precursors. Note the compaction of *scl* morphant cardiac discs in transverse optical sections as given in the insets of merged images (Fig. 4R). This phenotype was consistent with observations in *scl/tal1* mutant zebrafish where increased *cdh5* expression in aggregated endocardial precursors caused defective migration and disturbed anterior closure of the circular myocardium surrounding the endocardium (Bussmann et al., 2007). In *nkx2.5* morphants, we noticed an approximate 20% reduction in size of the *myl7*+ expression domain (Figures 4G and 4S). Consistent with the quantitation of *c3* transgene expression in *nkx2.5* knockdown embryos (Figure 3D), we observed spatial expansion of *c3* transgene expression domain (Figure 4H-I), further supporting the concept that loss of *nkx2.5* function resulted in a change of myocardial towards a more endothelial identity of these cells responding with increased expression of the *etv2* sequence-based reporter transgene. In contrast, endocardial precursors were unaffected by loss of *nkx2.5* function since cardiac *c2* transgene expression was unchanged (Figure 4S-U). Combined knockdown *scl* and *nkx2.5* resulted in a combined increase in *c3* transgene expression in both myo- and endocardial progenitor domains (Figure 4J-L). *C2* transgene expression was increased in endocardial cells as in *scl* single knockdown embryos, however when *nkx2.5* was knocked down concomitantly (Figure 4V-X), *myl7+c2* transgene co-expressing cells were also detected (see arrowhead in inset of Figure 4X). This indicated that *scl* and *nkx2.5* cooperated in transgene inhibition in myocardial progenitor cells. To quantify the degree of co-localization of *myl7* and respective transgene signals in control and morphant cardiac discs, we applied scatter plot analysis on the digitally reconstructed specimen (Fig. S6) in Volocity software. Scatter plots from green (*c3* and *c2* transgenes) and red (*myl7*) channels were generated from raw data of acquired z-stacks. Background correction in the region of interest (ROI i.e. cardiac disc, schematically indicated by blue dashed circles) resulted in threshold scatter plots enabling the calculation of co-localization (M_{red}, M_{green}) and overlap (R) coefficients. For the *c3* transgene, the overlap was maximal in the control morphant with R=77% and 83% of red pixels colocalizing with green pixels (M_{red}) and 72% of green pixels colocalizing with red pixels (Mgreen) in the cardiac disc ROI. In the *scl* morphant, the decrease in overlap between red and green channels (R=53%) and colocalization coefficients (M_{red}=65%, M_{green}=50%) indicated that the increase in *c3* transgene expression occurred in *myl7- "endocardial"* cells of the *scl* morphant cardiac disc. This finding was supported by the morphology of and central location of upregulated *c3* transgene expression in the *scl* morphant cardiac disc (Fig. 4D-F), and is consistent with the reported observations in *scl/ tal1* mutant zebrafish (Bussmann et al., 2007). According to our quantification of morphant embryo counts (Fig. 3D), the *nkx2.5* morphant cardiac disc also displayed an increase in *c3* transgene expression. However, the overlap and colocalization coefficients decreased only slightly compared to the control, and M_{green} (i.e. the percentage of c3+ signal colocalizing with *myl7*+ signal in the ROI) remained similar to the control (66% and 72%, respectively, as opposed to 50% and 72% for the *scl* knockdown), supporting the notion that *myl7+ "myocardial"* cells were the source of increased *c3* transgene expression in *nkx2.5*

morphants. A further reduction in colocalization and overlap coefficients in the *scl/nkx2.5* double morphant was consistent with further increased *c3* reporter expression according to our quantitation results (Fig. 3D). In contrast to a trend in reduction of colocalization and overlap coefficients for the *c3* transgene, we noticed a general trend towards an increase in colocalization between *c2* transgene and *myl7* signals upon both single *scl* and combined *scl/nkx2.5* knockdown. Single *nkx2.5* knockdown however had no effect on colocalization coefficients as compared to control morphant cardiac disc, supporting the idea that the role of *nkx2.5* in *etv2* inhibition is *scl*-dependent. In support of a previous report showing that endothelial specification overrides cardiac potential (Schoenebeck et al., 2007), we could not find any colocalization of endogenous *etv2* and *myl7* signals in double *scl/nkx2.5* morphant discs (data not shown). It is also noteworthy that cells outside the cardiac disc that are transgene-derived are also affected especially by *scl* knockdown (Figures 4E and 4Q), which supports the previous reported role for Scl in these vascular-derived structures (Gering et al., 2003; Patterson et al., 2005).

Taking the quantitative and co-localization data from the knockdown analysis of *c2* and *c3* transgene expression together, the results unambiguously point to *scl* and *nkx2.5* functioning as repressors of cardiac disc transgene (*etv2*) expression in cells destined to enter cardiac lineage at or after 6 som, and maintaining this repression at least until 22 som.

Modulation of *scl* and *nkx2.5* affects endogenous *etv2* expression in endocardial precursors

We next investigated whether *scl* and *nkx2.5* combined knockdown will affect endogenous *etv2* endocardial expression at cardiac disc/cone stages (Figure 5). Indeed, *scl/nkx2.5* double knockdown embryos (Figure 5A & B, p=0.045, n=91) showed more strong *etv2* expression compared to *scl* (Figure 5B) single knockdown morphants. The majority of the *etv2* expression modulation was however caused by *scl* knockdown since *nkx2.5* knockdown alone did not alter *etv2* expression significantly (Figure 5B, p=0.71, n=122 compared to std.ctrl-MO injection), thus correlating with intron-containing *c2* transgene knockdown responsiveness (Figure 3E-H). This indicated that the c2 transgene contained additional critical regulatory sequence to recapitulate the endogenous *etv2* expression pattern than the unregulated *c3* transgene. Taking the transgene and *etv2* expression modulation data together, we conclude that *scl* and *nkx2.5* are critical regulators of *etv2* expression in the developing zebrafish heart.

Etv2 intronic regions contain both repressive and enhancing cis-regulatory elements

To assess the contribution of sequence downstream of the transcription start site to *etv2* transcriptional regulation, we sought to quantify the *etv2* promoter activity using dual-luciferase reporter assays. A series of constructs were designed, and is shown in Figure 6A. To examine the influence of downstream sequence on promoter activity, we generated firefly luciferase-based reporter constructs harboring intron-less (c3) and intron-containing (c2) *etv2* promoter fragments (Figure 6A, c3 and c2). To exclude the effects of distance between the upstream promoter fragment and luciferase translation initiation region affecting reporter expression, we generated a control reporter construct that contained the downstream sequence in antiparallel orientation [c2(E1-I2)/anti]. After microinjection into

zebrafish zygotes, luciferase activity was assayed from whole zebrafish embryo lysates both at 6 and 22 somite stages (Figure 6B) to compare the impact of downstream sequence on *etv2* promoter activity in early versus late cardiovascular progenitor cells. Also, we analyzed promoter activity in a rat myocardium cell line (H9C2) post transfection of the constructs (Figure 6B). Constitutive Renilla luciferase expression driven by a weak thymidine kinase promoter served as an internal standard to normalize for transgenesis and transfection efficiency, respectively, and was co-injected or transfected with the respective firefly reporter constructs. Statistically significant differences in expression were calculated using *t*-tests. We observed that the intron-less c3 reporter showed high expression in zebrafish embryos at both 6 and 22 som without significant difference in time points (P=0.214). Relative to the empty vector, this upstream zebrafish *etv2* promoter fragment strongly induced reporter expression about 1000-fold (Figure 6B, c3-6 som and 22 som). Surprisingly, this fragment was also highly activated in mammalian embryonic myocardium cells, although one order of magnitude lower than in zebrafish embryos (Figure 6B, c3-H9C2). Because we observed ectopic activation of the analogous GFP reporter specifically in myocardial cells of the zebrafish cardiac disc [Figs. 1 and S2 (co-expression data)], this indicated functional and specific conservation of the intron-less *etv2* promoter activity in embryonic myocardium across species. The presence of downstream sequence resulted in strong reduction in reporter expression for the c2 reporter in both zebrafish embryos (100-fold) and rat H9C2 cells (10-fold) (Figure 6B, c2). Comparing 6 and 22 som stages, there was significantly more inhibition at 6 som than at 22 som for the *c2* reporter (P=0.017) indicating higher degree of repression of *etv2* promoter activity at 6 som in zebrafish. In the control situation where the downstream sequence was placed in antiparallel orientation [Figure 6B, c2(E1-I2/anti)], the difference in reporter expression between 6 and 22 som disappeared (P=0.900) indicating that temporal aspects of promoter activity were deregulated, and that the inhibition of the *etv2* promoter was dependent on the correct spatial orientation of putative cis-regulatory elements located in intronic downstream regulatory sequence. Strikingly, the c2(E1-I2/anti)-reporter displayed significantly less expression than the *c2* reporter (P=0.004) in H9C2 cells (Figure 6B, c2(E1-I2/anti) - H9C2) further supporting the notion that proper inhibition of promoter activity by downstream sequence was dependent on the spatial arrangement of regulatory elements in that sequence, and on the cellular context rather than simply the distance formed by nucleotides between the upstream promoter and translation start site of the reporter. Similarly, the expression of the c2(E1-I2/anti)-reporter was less than the c2-reporter at the 22 somite time point in zebrafish [Figure 6B, (*)]. Due to the in vivo nature of experiments using microinjections and analysis of heterogeneous whole embryo lysates as compared to homogenous H9C2 lysates, we think that this decrease was significant, although the t-test calculation showed this to be closely insignificant (P=0.068). In contrast, clearly no difference in promoter inhibition was observed between c2 and c2(E1-I2/anti) at 6 som (P=0.424), suggesting that the degree of *etv2* promoter inhibition was less flexible at early compared to late somitogenesis stages.

To eventually show that *etv2* promoter inhibition was independent of downstream sequence length, we replaced the downstream sequence by a neutral sequence that was putatively devoid of regulatory elements (Figure 6C). We selected combined protein coding sequence for ampicillin and kanamycin amplified from the pCR2.1-TOPO vector (Life Sciences) and

cloned it in antiparallel orientation between the upstream *c3* promoter fragment and the luciferase translation start (Figure 6A). Unexpectedly, replacement of the whole downstream region [c2-R(E1-I2)] resulted in similar reduction of reporter activity like the c2(E1-I2/anti)-reporter (Figure 6B) with loss of difference in reporter expression between 6 and 22 somite (Figure 6C, P=0.155, compared to difference in expression between these time points for c2 in this line of experiments with P=0.0098). This suggested that either the sequence length indeed played a role in general repression of the upstream *etv2* promoter region, or the replacement sequence was not as neutral as expected. To address these questions, we consecutively replaced both introns in the *etv2* downstream region by ampicillin/kanamycin coding sequence. Selective replacement of intron 1 [c2-R(I1)] resulted in clearly evident difference in expression between 6 and 22 som (Figure 6C, P=0.0002). No difference in reporter expression was observed at 6 som (P=0.1023), however, expression at 22 som increased two-fold on average (P=0.0075), both compared to the c2 reporter, indicating the presence of an inhibitory element located in intron 1, and that the element was inactive at 6 som. This result correlated with our previous observations that the absence of downstream sequence in the c3 (Kaede) reporter did not result in ectopic expression in myocardial (*nkx2.5*+) progenitor cells at the 6-8 som stage (Fig. S2), and the inability to significantly increase *c3* reporter expression by *scl/nkx2.5* knockdown in endothelial progenitor cells in the ALPM at 6-8 som (Fig. S3A and B). Selective replacement of intron 2 [c2-R(I2)] surprisingly resulted in almost complete absence of luciferase reporter expression at both 6 and 22 som stages compared to c2 (Figure 6C). These data indicated the existence of an enhancer element in the second intron of *etv2*. To investigate whether regulatory properties of *etv2* downstream sequence were conserved in a heterologous promoter context, we utilized the zebrafish *myl7* promoter, which was previously described in detail (Huang et al., 2003). Another series of constructs was generated as depicted in Figure 6D. We cloned the downstream *etv2* sequence in forward (myl7+(E1-I2)) and antiparallel (myl7+E1-I2/anti) orientation to the 3′ end of the *myl7* promoter and assayed luciferase activity in whole embryo lysates 24 h after microinjection (Figure 6E). The *myl7* promoter alone (myl7) induced luciferase expression around 8-fold relative to the empty vector, however the presence of the downstream sequence did not cause any change in *myl7* promoter activity. Surprisingly, when the sequence was attached in the antiparallel orientation, reporter expression was reduced about 3-fold (P=0.003) (myl7+(E1-I2), Figure 6E). This indicated that the degree of inhibition of *myl7* promoter activity was not affected by the insertion of sequence between the upstream promoter and luciferase translation start, but rather by the spatial arrangement of regulatory elements relative to the promoter. This result was consistent for both the *etv2* promoter in myocardial H9C2 cells and the *myl7* promoter in 24 hpf embryos indicating that elements in *etv2* downstream sequence could generally inhibit promoter activity. When the downstream *etv2* sequence was replaced by ampicillin/kanamycin-related sequence this inhibitory effect disappeared (myl7-R(E1-I2), Figure 6F). However, and in contrast to the *etv2* promoter, selective replacement of intron 1 did not result in de-repression of *myl7* promoter activity [myl7-R(I1)] but rather showed the opposite effect, indicating that the inhibitory element in intron 1 was inactive in the *myl7* promoter context. At this time, we are unable to explain the inhibitory feature of *etv2* downstream sequence in antiparallel orientation in myocardial cells or the *myl7* promoter. Consistent with a further increase in repression of *etv2* promoter activity upon replacement

of intron 2 [c2-R(I2), Figure 6C], *myl7* promoter activity was also almost completely diminished [myl7-R(I2), Figure 6F], which again indicated the presence of an enhancer element in intron 2. To assess this possibility, we placed the isolated intron 2 fragment upstream of the *myl7* promoter and observed around two-fold increase in *myl7* promoter activity (Figure 6F). This result was consistent with a similar increase in *etv2* promoter activity following replacement of intron 2 [Figure 6C, c2-R(I2)], thus confirming general promoter enhancing activity in intron 2.

Taking all results of luciferase assays together, the data suggest that at least two cis-regulatory elements control the expression of *etv2*: one element located in intron 1 is important for inhibition of *etv2* at cardiac disc/cone stages, and intron 2 contains another element providing positive input into the locus to support *etv2* expression during both early and late somitogenesis stages.

Scl binds to zebrafish *etv2* proximal promoter DNA in vitro

Since *scl* knockdown resulted in an increase in both intron-less and intron-containing reporter transgene as well as endogenous *etv2* expression in heart progenitor cells, we investigated whether Scl directly binds to the *etv2* promoter. Several putative consensus-binding sites (E-boxes) for bHLH transcription factors were found in the *etv2* promoter region using MatInspector binding site prediction software. Binding sites for NKX transcription factor proteins flank an E-box (-281 to -276 relative to the transcription start site of *etv2*) (Figure S1C). It is well established that Scl binds to its cognate DNA targets in heterodimeric complexes with class A bHLH proteins E12 and E47 (Hsu et al., 1994) products of the *tcf3* gene in zebrafish. We performed electromobility shift assays (EMSA) to assess the possibility that Scl binds to the predicted E-box motif (Figure 7). Scl and Tcf3 proteins were produced in reticulocyte-based TNT lysate with PCR-generated DNA templates (Figure 7A). Both proteins were FLAG-tagged and co-expressed in TNT lysate (ST-lysate in Figure 7B). Western blot was performed to confirm protein expression using anti-FLAG antibody (left lane in Figure 7A, compare to single expressions on the right side of the marker lane). TNT-lysates were incubated with radioactively end-labeled dsDNA probes containing the E-box motif (WT probe). After separation in a non-denaturing polyacrylamide gel, an additional band was detected (lane 3, indicated by black arrowhead), which was absent after incubation of the WT probe and lysate processed with water instead of PCR template (W-lysate in Figure 7B, lane 2) or WT probe incubated in binding buffer only (lane 1). This indicated that in-vitro-translated Scl and Tcf3 proteins bound the E-box motif DNA. To determine if the formation of this protein-DNA complex was sequence-specific, competition assays were performed. The presence of increasing amounts of unlabeled WT probes (WT competitor, 200 and 540 ng, lanes 4 and 5, respectively) in the binding reaction resulted in a dose-dependent decrease in complex detection. The display of complex formation was almost abolished after the addition of 540 ng WT competitor to the binding reaction. In contrast, increasing equivalent amounts of competitor DNA containing a mutated E-box motif (transversions) only had a minimal effect on complex formation (mut competitor, lanes 6 and 7), and the complex was still clearly visible after addition of 540 ng mutant competitor (lane 5 compared to 7). Complex formation was absent using a labeled mutant probe with either with ST-lysates (lanes 8 and 9) or W-lysates (lanes 10 and 11).

Note the formation of unspecific complexes by undefined lysate components whose intensities were not affected by the addition of competitor DNAs (indicated by white stars in Figure 7B). Free WT and mutant probes were displayed in absence of lysate (lanes 1, 12 and 13). The presence of anti-FLAG antibody in the binding reaction caused the disappearance of the complex in a supershift assay (Figure S7, compare lane 5 with lanes 6 and 7, marked by arrowhead). The intensity of signal in and just below the loading pockets increased in presence of antibody (Figure S7, compare lanes 5 and 6/7, marked by + and *, respectively) indicating the supershifted complex in that location. This result confirmed that recombinantly expressed and FLAG-tagged Scl and E12/47 proteins interacted with the E-box motif of the probe. Together, our biochemical data show that Scl and Tcf3 proteins bind sequence-specifically to the predicted E-box motif in the proximal *etv2* promoter in vitro, providing evidence for a direct physical interaction of Scl with the *etv2* promoter to inhibit *etv2* gene expression in endocardial progenitor cells.

Discussion

In this study, we report the genomic plasticity of the *etv2* locus in that elements within the locus direct tissue-specific activator and repressor activities during endocardial and myocardial cell development. The salient features of this study include the identification of intronic elements in the *etv2* genomic locus that are responsible for repressing *etv2* transcription in myocardial and endocardial precursor cells, the role of Scl and Nkx2.5 transcription factors in maintaining this repression, and the plasticity of the *etv2* locus as demonstrated by the identification of enhancer and repressor sequences located in the first two introns of *etv2*.

The current knowledge of how myocardial, endocardial and endothelial lineages are derived from progenitor cells in zebrafish embryo is not well understood. Fate-mapping studies have demonstrated that during early gastrulation, cardiac progenitors arise from bilateral cell populations of the anterior lateral plate mesoderm (ALPM). Further, myocardial and endocardial progenitors originate in different spatial regions, and are separated (Keegan et al., 2004; Lee et al., 1994). The transcription factor networks that guide this process are poorly understood. Etv2, a key regulator of vascular endothelial cell differentiation is expressed in endothelial and endocardial but not in myocardial cells (Proulx et al., 2010). This suggests that the regulation of *etv2* expression in progenitor cells is likely to influence subsequent steps of cardiac lineage differentiation. We cloned upstream genomic elements in the *etv2* locus that might be responsible for this regulation, and noticed a clear difference in the reporter expression between two transgenic lines, one harboring an intron-containing element (c2) and an intron-deleted element (c3). *C2* and *c3* reporters co-localize with endogenous *etv2* expression until 8 som but at some point in between 8 and 20 som, we notice *c3* expression switches into myocardial progenitors. If this switch in reporter expression is functionally related to the loss of repressor element in the intron sequence, our results imply that cells of myocardial and endocardial lineages are plastic between 8 and 20 som stages. Previous data has suggested that *etv2* is never expressed in myocardial progenitor cells and the two lineages have already separated at the one-somite stage when the *etv2* expression is initiated within the ALPM (Palencia-Desai et al., 2011). Our results are consistent with this interpretation in that *etv2* expression is repressed in myocardial

progenitor cells. However, the timing of separation of these lineages is not consistent with our findings, which is more accurately determined with RNA expression analysis as performed here compared to GFP protein fluorescence analysis (Palencia-Desai et al., 2011). Beyond 22 som, the c2 reporter mimics the endogenous *etv2* expression pattern and is not detectable after 36 hpf, while the c3 reporter continues to express in the zebrafish heart at 40 hpf and beyond indicating both a spatial and temporal misregulation of the transgene (Figure S3). The data from luciferase-based promoter analysis provide additional supportive evidence in that a critical cis-regulatory element resides in *etv2* intronic sequence. This element most likely complement elements in promoter sequence located upstream of the TSS, and is dispensable at 6 som but essential at 22 som in repressing the reporter. Collectively, these results suggest that post 8 som and before 20 som, the *etv2* expression is repressed in a select group of cells, which may retain bipotential (endocardial and myocardial lineage) ability. Studies in zebrafish that show vessel and blood specification overriding cardiac potential in ALPM (Schoenebeck et al., 2007) support the multipotential nature of cardiac precursor cells.

What is the mechanism of *etv2* repression in cardiac progenitor cells? Cardiac-specific transcription factors Nkx2.5, Gata5, and Scl are likely to participate in this mechanism. Nkx2.5 is one of the earliest markers of myocardial differentiation, and is observed in bilateral ALPM as early as 10 som stage (Goldstein and Fishman, 1998), and these cells merge in the midline at 20 som. Knocking down *nkx2.5* and *scl* in tandem clearly induces reporter transgene expression in both c2 and c3 transgenic lines, with a statistically significant increase in c3 (Figure 3D, p=2.746e-007) compared to *c2* transgene expression. Interestingly, the identities of cell types that express the reporter transgene in these double knockdowns provide some insight. In the c3 line, combined knockdown of *scl* and *nkx2.5* increased *c3* transgene expression in both myo- and endocardial progenitor domains (Figure 4J-L). In the c2 line, reporter gene expression was increased in endocardial cells as in *scl* single knockdown embryos, however when *nkx2.5* was knocked down concomitantly (Figure 4V-X), we detected *myl7+ c2* reporter co-expressing cells (see arrowhead in inset of Figure 4X) indicating that *scl* and *nkx2.5* cooperated in transgene inhibition in myocardial progenitor cells. More importantly, *nkx2.5* and *scl* modulate endogenous *etv2* expression in the endocardium at 20 som. Taken together, this argues for a previously unappreciated role for *nkx2.5* to act as a functional repressor of the *etv2* locus perhaps in putatively myocardial leaning progenitor cells after initial specification events. Further, this repressive function of *nkx2.5* is *scl*-dependent, since *nkx2.5* knockdown alone did not significantly alter *c2* transgene or endogenous *etv2* expression. However, *nkx2.5* knockdown alone did alter *c3* transgene expression, which is most likely explained by the lack of critical regulatory sequences in c3 that is required for prevention of ectopic *etv2* activation in the myocardial lineage by *nkx2.5* or downstream effectors. Whether transcriptional changes alone in *etv2* locus or alternative hypothesis such as cell fate changes in *nkx2.5* knockdown embryos explains the observed effect remains to be decided. *Nkx2.5* knockdown may indeed alter cell fates early based on recent publication indicating that *nkx2.5* (and *nkx2.7*) is required to maintain ventricular versus atrial myocardium identities following initial specification of precursor populations (Targoff et al., 2013). Consistently, in *nkx2.5* knockdown embryos, we do not observe significant increase in c3 or c2 expression at 6-8 som. In contrast, in later

embryos (22 som), *nkx2.5* loss in c3 (intron-less line) clearly showed increased c3 expression in cardiac (Fig. S4A) and also head vessel progenitors (Fig. S4B) but minimal effects were observed in posterior vessel progenitors (Fig. S4C). This suggests selectivity in Nkx2.5's effects on cell populations at LPM. A cell-autonomous role for Nkx2.5 in establishing gene-expression borders within myocardial populations via Notch pathway has been shown recently (Nakashima et al., 2014). Our data that loss of *nkx2.5* function lead to increased c3 expression in *nkx2.5* negative head vessel progenitor cells may even point to a non-cell autonomous role for Nkx2.5 in maintenance of LPM-derived cardiac and endothelial lineages. However, Nkx2.5's function in a common progenitor cell cannot be fully excluded. From a transcriptional mechanism standpoint, the downstream intronic *etv2* sequence functions later, and is essential to limit *etv2* expression in anterior LPM-derived structures. This is based on results from co-expression (Fig. 2, S2 and 4), knockdowns (Fig. 3, S3 and S4), and luciferase (Fig. 6) assays. Similar to *nkx2.5*, knocking down *etv2* and *scl* together showed more embryos with strong transgene expression in the cardiac domain (Figure 3B4, p=0.004) compared to knocking down *etv2* alone indicating that Scl but not Etv2 regulated *c3* transgene expression. Interestingly, previous studies have shown that knocking down *etv2* alone results in abrogation of trunk LPM *scl* cells (Sumanas and Lin, 2006) at 6 and 10 som, implying that Scl-Etv2 transcription factors are dynamically controlling population of cells at LPM with perhaps trunk LPM cells programmed for vascular fate specification, and the ALPM population for cardiac specification. Collectively, the emerging theme here is that *etv2* expression during cardiac progenitor cell development is co-regulated by transcription factor pairs (Scl & Etv2, Nkx2.5 & Scl), and perhaps Scl plays a critical “molecular switch” role. This hypothesis would predict that Scl functions as an activator in vascular cell fate, and a repressor in cardiac cell fate. Indeed, in mouse Scl represses cardiomyogenesis in prospective hemogenic endothelium and endocardium (Van Handel et al., 2012). In *scl/tal1* zebrafish mutants, endocardial precursors at cardiac disc stages show selective defective migration (Bussmann et al., 2007), and an increase in *cdh5+* endocardial cells. *Cdh5* is a putative direct transcriptional target of *etv2* (De Val et al., 2008), and *etv2* upregulation in endocardial precursors due to Scl loss-of-function could explain the increase in *cdh5+* cells in this mutant. These examples and our EMSA data of Scl direct interaction with the *etv2* promoter supports the idea that Scl functions as an *etv2* repressor in endocardial progenitor cells. Other factors such as Gata5 may also participate in this regulation. *Gata5* functionally counteracts the effects of *nkx2.5* in the *etv2* locus perhaps in driving cells towards endocardial lineage. *Gata5* is known to function as an activator in cardiogenic precursor cells where it synergistically works with NF-ATc to activate endocardial transcription (Nemer and Nemer, 2002).

Our data suggests a dynamic *etv2* genomic locus that undergoes changes during the distinct steps of cardiovascular development. The intronic cis-regulatory elements in *etv2* cooperate with the upstream promoter region to effectively regulate *etv2* expression in that the elements convey the correct transcriptional output of *etv2* by integration of (*nkx2.5*-, *gata5*-mediated) extrinsic and (*scl*-, *etv2*-mediated) intrinsic cues. In turn, these cues control the responsiveness of *etv2* cis-regulatory elements to changing environments during different stages of cardiovascular development. At earlier 6-8 somite stages, the spatial arrangement and gene expression environment of ALPM precursors is substantially different. Here,

nkx2.5+ progenitor cells are located in the most posterior portion of the ALPM, thus still spatially separate from *etv2*+ endothelial/endocardial progenitors, *scl* is robustly expressed in *etv2*+ cells, and thus *etv2* intronic sequence may be dispensable to prevent its misexpression in *nkx2.5*+ progenitor cells. It is possible that the identified *etv2* intronic elements become more significant when initially specified endocardial and myocardial progenitor cells migrate to the embryonic midline and undergo complex morphogenetic movements during cardiac disc formation and elongation (Bussmann et al., 2007). During these stages, inter-cellular signals between endocardial and myocardial progenitors may be important to dynamically regulate *etv2* transcription. Intronic sequence then shields the *etv2* locus from *nkx2.5* [and redundant *nkx2.7* (Targoff et al., 2013)] function in myocardial and neighboring progenitors, and Scl directly inhibits *etv2* in endocardial progenitors concomitantly. In addition, activation of *etv2* occurs in endothelial precursors through enhancer elements *up1* [targeted by Foxc transcription factors (Veldman and Lin, 2012)] and in intron 2 (this study) probably through an ETS factor mediated positive feedback loop. Consistent with an important role for *nkx2.5* in establishing gene expression borders between myocardial-derived linages through the Notch pathway (Nakashima et al., 2014), it is conceivable that *nkx2.5* provides non-cell autonomous cues that ensure endothelial and cardiac lineage separation between endocardial and myocardial lineages during cardiac disc to elongation stages. These Nkx2.5 roles are in addition to its role in maintenance of ventricular-myocardial identity. Support to this notion comes from our observation that loss of *nkx2.5* not only increased cardiac, but also head vessel expression of the *c3* transgene. Other mechanisms that may contribute to *etv2* repression include the recent identification of microRNA coding elements in the 3′UTR of *etv2* (Moore et al., 2013), which adds another layer of *etv2* regulation at this locus. Future studies will illuminate the details of these seemingly disparate mechanistic processes, and whether these mechanisms are amenable to therapeutic manipulations that will benefit cardiovascular disease.

In summary, this study has identified novel elements in *etv2* cis-regulatory sequence that are partly responsible for mediating inhibition of *etv2* expression via Nkx2.5 and Scl transcription factors. These elements and factors help maintain the repressive state of the *etv2* genomic locus in cardiac progenitor cells thus implying the existence of endothelial progenitors with endocardial and myocardial lineage plasticity and expanding the concept of cardiogenic endothelium. To our knowledge, this is the first report that links Scl and Nkx2.5 transcription factors in a novel cis-regulatory repression mechanism during embryonic cardiac development of vertebrates.

Conclusions

Recently, the existence of multipotent progenitors of cardiac, blood and endothelial cell lineages was proposed. Genes essential for blood and endothelial specification were shown to restrict the cardiac potential of progenitor cells, however, the molecular mechanisms underlying the separation and maintenance of cardiovascular lineages remain unclear. Here, we identify a cis-regulatory mechanism controlling expression of *etv2*, a transcription factor essential for endothelial cell identity and shown to participate in blood and cardiac lineage specification decisions during zebrafish embryonic development. In particular, mechanisms preventing *etv2* expression in cardiac progenitor cells are unknown. We identified *etv2*

genomic elements precluding *etv2* misexpression in cardiac progenitor cells, and this regulation occurs between 8 and 22 somite stages in the developing zebrafish embryo. Further we found that *scl* and *nkx2.5*, genes important for blood and cardiac specification, work cooperatively to inhibit *etv2* expression, and this co-regulation is functionally responsible for myocardial and endocardial progenitor cell population development in the cardiac disc. Our results confirm the recently recognized developmental plasticity of cardiovascular progenitor cells during development.

Supplementary Material

Refer to Web version on PubMed Central for supplementary material.

Acknowledgments

We thank Pippa Simpson, PhD for statistical analysis, Suresh Kumar, PhD for assistance in confocal imaging, and Chris Koceja for technical assistance. Financial support for this work was provided by NIH grants HL090712, HL102745 and HL112639 to RR, and by seed funds from the Children's Research Institute at the Medical College of Wisconsin, Milwaukee to R.R. The funders had no role in the study design, the collection, analysis and interpretation of data. M.S. designed and performed experiments, analyzed data and wrote the paper; M.W. designed and performed experiments; C.Z.C. provided intellectual input and assisted in data interpretation, and R.R. designed experiments, analyzed data and wrote the paper.

References

Brown LA, Rodaway AR, Schilling TF, Jowett T, Ingham PW, Patient RK, Sharrocks AD. Insights into early vasculogenesis revealed by expression of the ETS-domain transcription factor Fli-1 in wild-type and mutant zebrafish embryos. Mechanisms of development. 2000; 90:237–252. [PubMed: 10640707]

Bussmann J, Bakkers J, Schulte-Merker S. Early endocardial morphogenesis requires Scl/Tal1. PLoS genetics. 2007; 3:e140. [PubMed: 17722983]

Chun CZ, Remadevi I, Schupp MO, Samant GV, Pramanik K, Wilkinson GA, Ramchandran R. Fli+ etsrp+ hemato-vascular progenitor cells proliferate at the lateral plate mesoderm during vasculogenesis in zebrafish. PLoS ONE. 2011; 25:e14732. [PubMed: 21364913]

De Val S, Chi NC, Meadows SM, Minovitsky S, Anderson JP, Harris IS, Ehlers ML, Agarwal P, Visel A, Xu SM, Pennacchio LA, Dubchak I, Krieg PA, Stainier DY, Black BL. Combinatorial regulation of endothelial gene expression by ets and forkhead transcription factors. Cell. 2008; 135:1053–1064. [PubMed: 19070576]

Gering M, Rodaway AR, Gottgens B, Patient RK, Green AR. The SCL gene specifies haemangioblast development from early mesoderm. The EMBO journal. 1998; 17:4029–4045. [PubMed: 9670018]

Gering M, Yamada Y, Rabbitts TH, Patient RK. Lmo2 and Scl/Tal1 convert non-axial mesoderm into haemangioblasts which differentiate into endothelial cells in the absence of Gata1. Development. 2003; 130:6187–6199. [PubMed: 14602685]

Goldstein AM, Fishman MC. Notochord regulates cardiac lineage in zebrafish embryos. Dev Biol. 1998; 201:247–252. [PubMed: 9740662]

Holtzinger A, Evans T. Gata5 and Gata6 are functionally redundant in zebrafish for specification of cardiomyocytes. Dev Biol. 2007; 312:613–622. [PubMed: 17950269]

Hsu HL, Huang L, Tsan JT, Funk W, Wright WE, Hu JS, Kingston RE, Baer R. Preferred sequences for DNA recognition by the TAL1 helix-loop-helix proteins. Molecular and cellular biology. 1994; 14:1256–1265. [PubMed: 8289805]

Huang CJ, Tu CT, Hsiao CD, Hsieh FJ, Tsai HJ. Germ-line transmission of a myocardium-specific GFP transgene reveals critical regulatory elements in the cardiac myosin light chain 2 promoter of zebrafish. Dev Dyn. 2003; 228:30–40. [PubMed: 12950077]

Keegan BR, Meyer D, Yelon D. Organization of cardiac chamber progenitors in the zebrafish blastula. Development. 2004; 131:3081–3091. [PubMed: 15175246]

Lee RK, Stainier DY, Weinstein BM, Fishman MC. Cardiovascular development in the zebrafish. II. Endocardial progenitors are sequestered within the heart field. Development. 1994; 120:3361–3366. [PubMed: 7821208]

Link V, Shevchenko A, Heisenberg CP. Proteomics of early zebrafish embryos. BMC developmental biology. 2006; 6:1. [PubMed: 16412219]

Manders EMM, Verbeek FJ, Aten JA. Measurement of co-localization of objects in dual-colour confocal images. Journal of Microscopy. 1993; 169:375–382.

Moore JC, Sheppard-Tindell S, Shestopalov IA, Yamazoe S, Chen JK, Lawson ND. Post-transcriptional mechanisms contribute to Etv2 repression during vascular development. Dev Biol. 2013; 384:128–140. [PubMed: 24036310]

Nakashima Y, Yanez DA, Touma M, Nakano H, Jaroszewicz A, Jordan MC, Pellegrini M, Roos KP, Nakano A. Nkx2-5 suppresses the proliferation of atrial myocytes and conduction system. Circ Res. 2014; 114:1103–1113. [PubMed: 24563458]

Nemer G, Nemer M. Cooperative interaction between GATA5 and NF-ATc regulates endothelial-endocardial differentiation of cardiogenic cells. Development. 2002; 129:4045–4055. [PubMed: 12163407]

Palencia-Desai S, Kohli V, Kang J, Chi NC, Black BL, Sumanas S. Vascular endothelial and endocardial progenitors differentiate as cardiomyocytes in the absence of Etsrp/Etv2 function. Development. 2011; 138:4721–4732. [PubMed: 21989916]

Patterson LJ, Gering M, Eckfeldt CE, Green AR, Verfaillie CM, Ekker SC, Patient R. The transcription factors Scl and Lmo2 act together during development of the hemangioblast in zebrafish. Blood. 2007; 109:2389–2398. [PubMed: 17090656]

Patterson LJ, Gering M, Patient R. Scl is required for dorsal aorta as well as blood formation in zebrafish embryos. Blood. 2005; 105:3502–3511. [PubMed: 15644413]

Peterkin T, Gibson A, Patient R. Common genetic control of haemangioblast and cardiac development in zebrafish. Development. 2009; 136:1465–1474. [PubMed: 19297410]

Pham VN, Lawson ND, Mugford JW, Dye L, Castranova D, Lo B, Weinstein BM. Combinatorial function of ETS transcription factors in the developing vasculature. Dev Biol. 2007; 303:772–783. [PubMed: 17125762]

Proulx K, Lu A, Sumanas S. Cranial vasculature in zebrafish forms by angioblast cluster-derived angiogenesis. Dev Biol. 2010; 348:34–46. [PubMed: 20832394]

Reichenbach B, Delalande JM, Kolmogorova E, Prier A, Nguyen T, Smith CM, Holzschuh J, Shepherd IT. Endoderm-derived Sonic hedgehog and mesoderm Hand2 expression are required for enteric nervous system development in zebrafish. Dev Biol. 2008; 318:52–64. [PubMed: 18436202]

Schoenebeck JJ, Keegan BR, Yelon D. Vessel and blood specification override cardiac potential in anterior mesoderm. Dev Cell. 2007; 13:254–267. [PubMed: 17681136]

Sumanas S, Lin S. Ets1-related protein is a key regulator of vasculogenesis in zebrafish. PLoS biology. 2006; 4:e10. [PubMed: 16336046]

Targoff KL, Colombo S, George V, Schell T, Kim SH, Solnica-Krezel L, Yelon D. Nkx genes are essential for maintenance of ventricular identity. Development. 2013; 140:4203–4213. [PubMed: 24026123]

Targoff KL, Schell T, Yelon D. Nkx genes regulate heart tube extension and exert differential effects on ventricular and atrial cell number. Dev Biol. 2008; 322:314–321. [PubMed: 18718462]

Thattaliyath BD, Firulli BA, Firulli AB. The basic-helix-loop-helix transcription factor HAND2 directly regulates transcription of the atrial naturetic peptide gene. Journal of molecular and cellular cardiology. 2002; 34:1335–1344. [PubMed: 12392994]

Thisse C, Thisse B. High-resolution in situ hybridization to whole-mount zebrafish embryos. Nature protocols. 2008; 3:59–69.

Trinh LA, Yelon D, Stainier DY. Hand2 regulates epithelial formation during myocardial diferentiation. Current biology : CB. 2005; 15:441–446. [PubMed: 15786591]

Van Handel B, Montel-Hagen A, Sasidharan R, Nakano H, Ferrari R, Boogerd CJ, Schredelseker J, Wang Y, Hunter S, Org T, Zhou J, Li X, Pellegrini M, Chen JN, Orkin SH, Kurdistani SK, Evans SM, Nakano A, Mikkola HK. Scl represses cardiomyogenesis in prospective hemogenic endothelium and endocardium. Cell. 2012; 150:590–605. [PubMed: 22863011]

Veldman MB, Lin S. Etsrp/Etv2 is directly regulated by Foxc1a/b in the zebrafish angioblast. Circ Res. 2012; 110:220–229. [PubMed: 22135404]

Zinchuk V, Zinchuk O, Okada T. Quantitative colocalization analysis of multicolor confocal immunofluorescence microscopy images: pushing pixels to explore biological phenomena. Acta histochemica et cytochemica. 2007; 40:101–111. [PubMed: 17898874]

Highlights

The genomic locus in *etv2* responsible for cardiac progenitor cell specification is unknown. Our work sheds some light on this problem, and is the first to report:

- On a dynamic cis-regulatory mechanism to restrict *etv2* function
- Proximal promoter sequences that prevents *etv2* misexpression in cardiac cells
- *Scl* and *nkx2.5* inhibit cardiac *etv2* expression
- Nkx2.5's role in cardiac repression mechanism is Scl-dependent, and
- Identification of intronic elements responsible for the *etv2* regulation

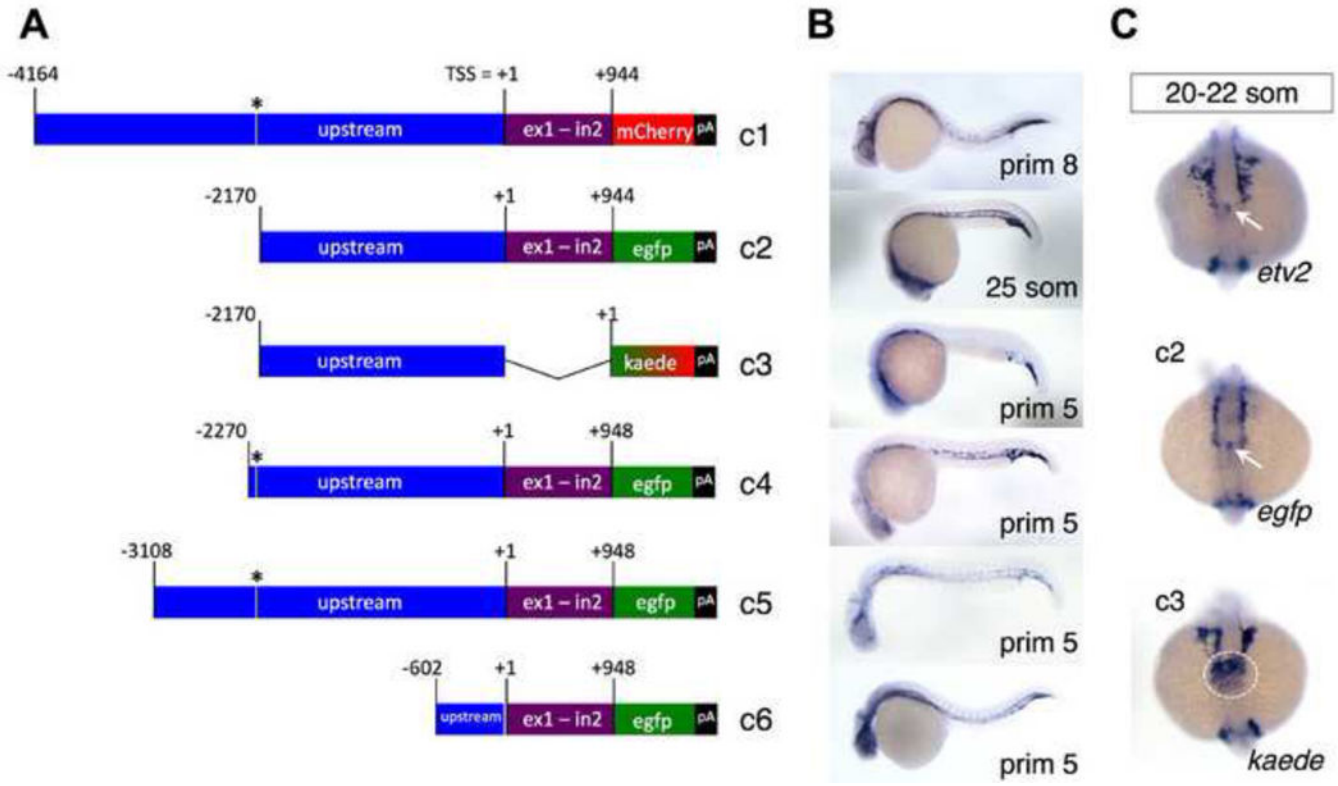

Figure 1. Overview on transgenic construct designs and expression patterns

(A) Constructs c1-c6 contained different fragments of the *etv2* locus on chromosome 16 ranging from inclusion of the whole non-coding 4164 bp *etv2-fli1b* intergenic region (blue) plus the first and second exon-intron pair (purple) downstream of the transcription start site (TSS) fused to cDNA of fluorescent reporter protein *mCherry* in c1, a shorter 2170 bp upstream fragment plus the downstream region fused to *egfp* cDNA in c2, and a 2170 bp upstream fragment without the downstream exon-intron pair fused to *kaede* coding sequence in c3. Construct c4 contained 100 bp more upstream sequence than c2 including the FOXC binding site (black asterisks) described by (Veldman and Lin, 2012), and c5 and c6 contained 3108 bp and 602 bp upstream sequence, respectively. C4-c6 also included the downstream region (equivalent to c1 and c2), and was fused to the *egfp* reporter. All constructs c1-c6 contained a polyadenylation signal (pA) at the 3′ end. **(B)** Expression patterns of c1-c6 in stable transgenic embryos around 1 dpf (25 som to prim 8 stages) were revealed by ISH. Representative embryos are oriented laterally with the head to the left. All transgenes showed robust vascular expression in head and axial vessels and the vascular plexus region recapitulating the endogenous *etv2* expression pattern except for c3, which showed vascular plexus expression but reduced axial and head vessel expression. **(C)** At 20-22 som, endogenous *etv2* expression is present in the endocardial domain of the developing cardiac disc, which was recapitulated by the c2 *egfp* reporter (white arrows). In contrast, the c3 *kaede* reporter was expressed in the myocardial domain of the early heart (white dashed circle). Embryo views are dorsal with the head to the top.

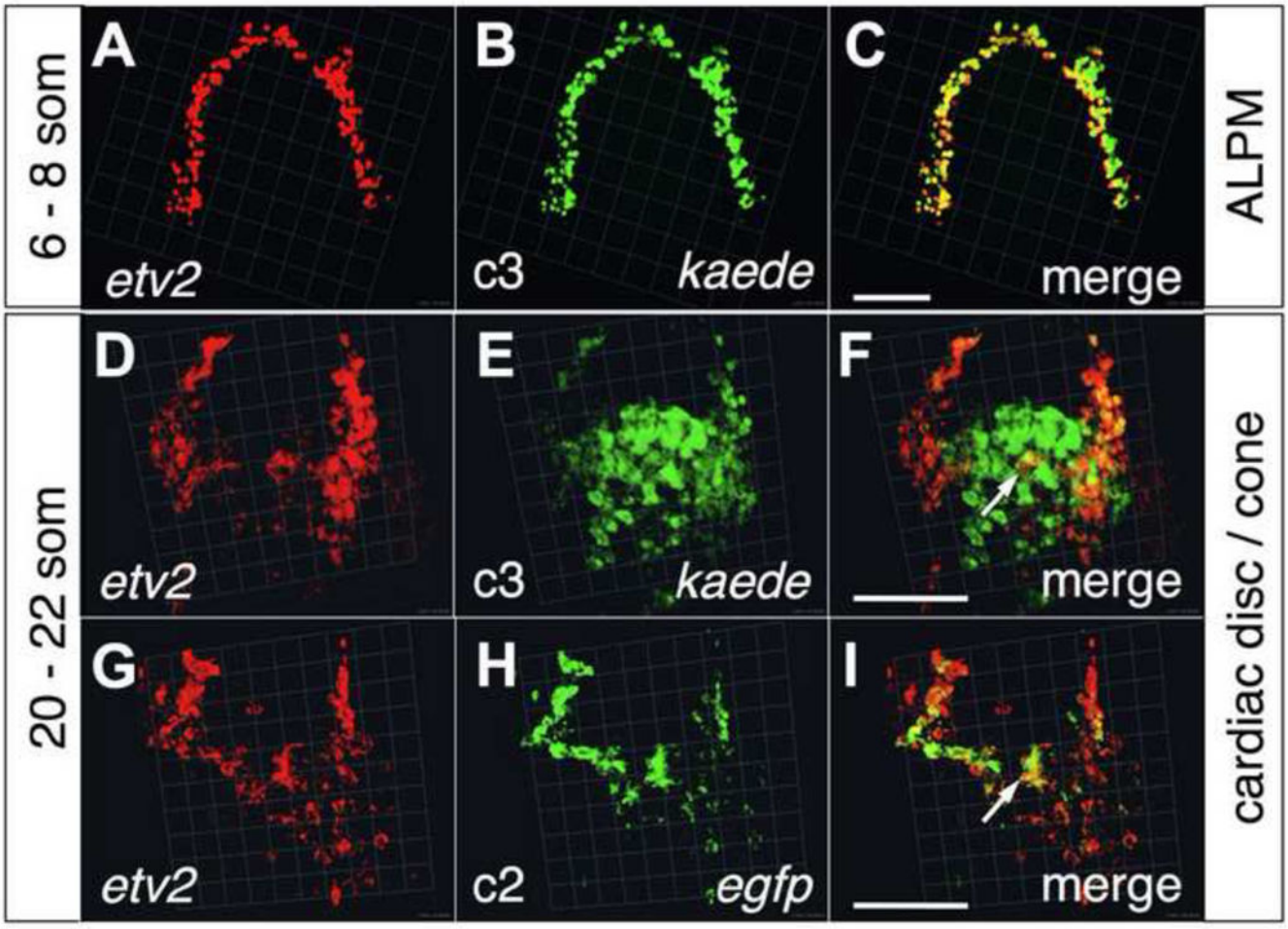

Figure 2. The c3 intron-less reporter recapitulates endogenous *etv2* expression pattern during early but not late segmentation stages

Two-color fluorescent ISH of c3 transgenic embryos at 6-8 som in the ALPM (**A-C**) and at 20-22 som in the cardiac disc (**D-F**) for the detection of endogenous transcripts of *etv2* in red (**A & D**) and concomitant detection *of kaede* transcripts from the *c3* transgene in green (**B & E**), merged in (**C & F**). At 6-8 som, maximal overlap of both signals was observed (**C**), however at 20-22 som, cardiac *c3* transgene expression did not overlap with endogenous *etv2* (**F**) whereas the c2 *egfp* transgene recapitulated *etv2* expression at that stage (**G-H**). Embryos are dorsal with anterior to the top. Images shown are snapshots from 3D views with bars ≈100 μm related to the background grid (1 unit = 45.18 μm in A-C, 22.59 μm in D-F, and 22.54 μm in G-I)

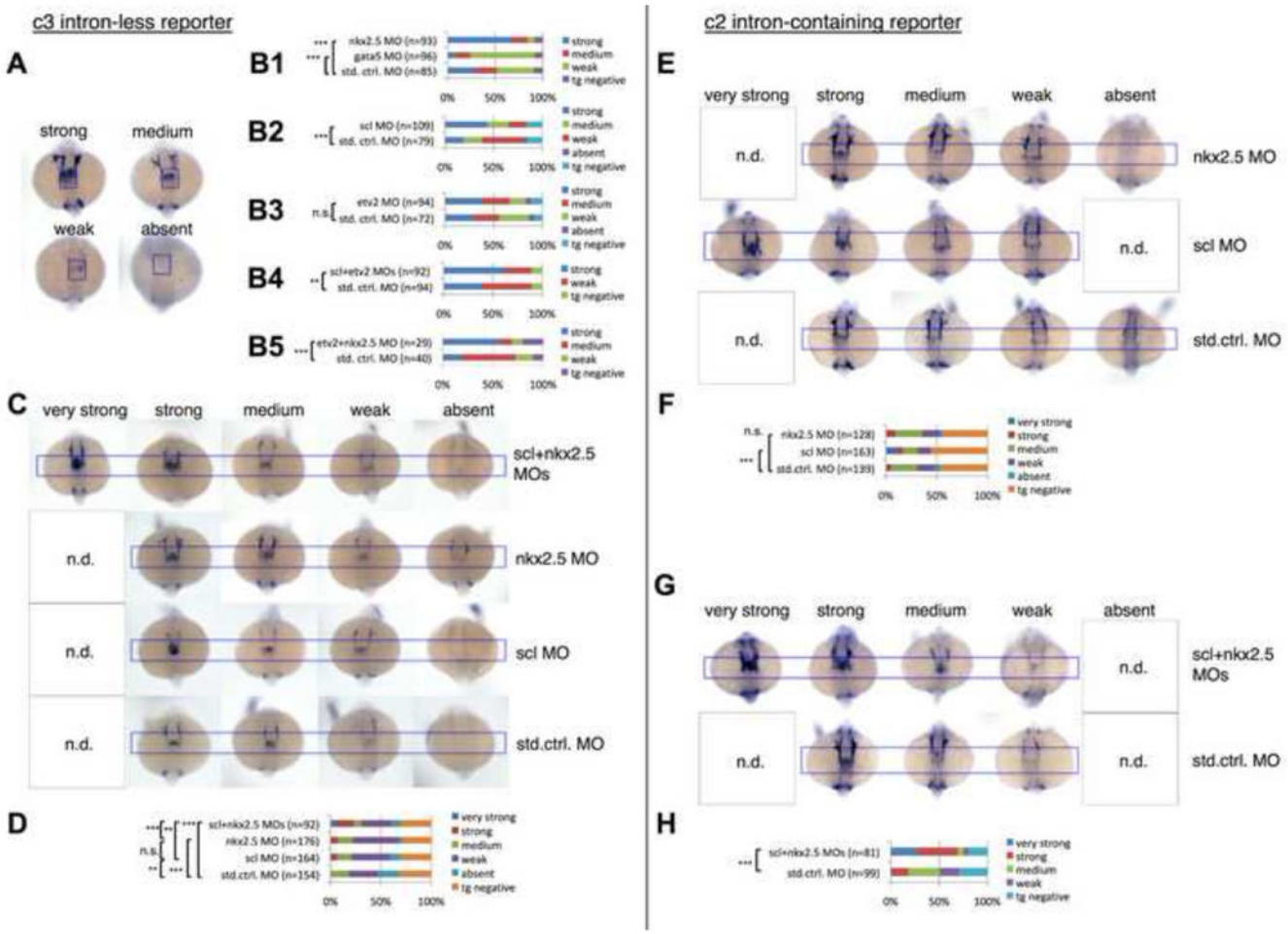

Figure 3. Changes in intron-less *c3* transgene versus intron-containing *c2* transgene expression magnitudes in the cardiac disc in response to single and combined knockdowns of key myocardial *(gata5, nkx2.5*) and endocardial/endothelial (*scl, etv2*) transcription factors

(A) Representative embryos post ISH showing four categories of *c3* transgene expression magnitudes in the myocardial domain of the cardiac disc (blue frame) with transgene expression categories scored and quantified in **(B1-5)**. Knockdown of *nkx2.5* resulted in an increase, knockdown of *gata5* in a decrease of c3 transgene expression (**B1**). Knockdown of *scl* also lead to an increase **(B2)**, *etv2* morphants however showed no significant change in c3 transgene expression **(B3)**. Combined knockdown of *scl* and *etv2* **(B4)** or *nkx2.5* and *etv2* **(B5)** again resulted in increased c3 transgene expression indicating that *scl* and *nkx2.5* (but not *etv2*) cooperate in c3 repression. **(C-D)** Combined knockdown of *scl* and *nkx2.5* compared to single knockdowns showing cardiac disc expression categories of the c3 transgene in representative embryos **(C)** and quantification **(D)**. Note that combined *scl* and *nkx2.5* knockdown resulted in an additional category of “very strong” c3 transgene expressing embryos not seen in single knockdowns indicating synergism of *scl* and *nkx2.5* in c3 transgene repression. **(E)** Representative embryos showing categories of c2 transgene expression in the endocardial domain of the cardiac disc following single knockdowns of *scl* and *nkx2.5* and quantification in **(F)**. **(G)** Combined knockdown of *scl* and *nkx2.5* showing cardiac disc expression categories of the c2 transgene in representative embryos and

quantification in **(H)**. Note that single *nkx2.5* knockdown resulted in significant change in c3 but not c2 transgene expression (compare **D** and **F**). Embryos shown are at 20-22 som stages in dorsal view with anterior to the top. *** indicates p≤0.001; ** indicates p≤0.01; * indicates p≤0.05; n.s.=not significant (p>0.05); n.d.=not detected; MO=morpholino; n=number of scored embryos; blue frame marks the endocardial cardiac disc expression domain of the *c2* transgene. Categories of transgene expression magnitudes scored are color-coded in **(B, D, F & H)**. Pooled F2 and F3 generations of two transgenic c3 lines were analyzed in **A/B**, and pooled F5 and F2 generations of 2 lines in **C/D**. F4 generation embryos of two c2 lines were analyzed in **E-H**.

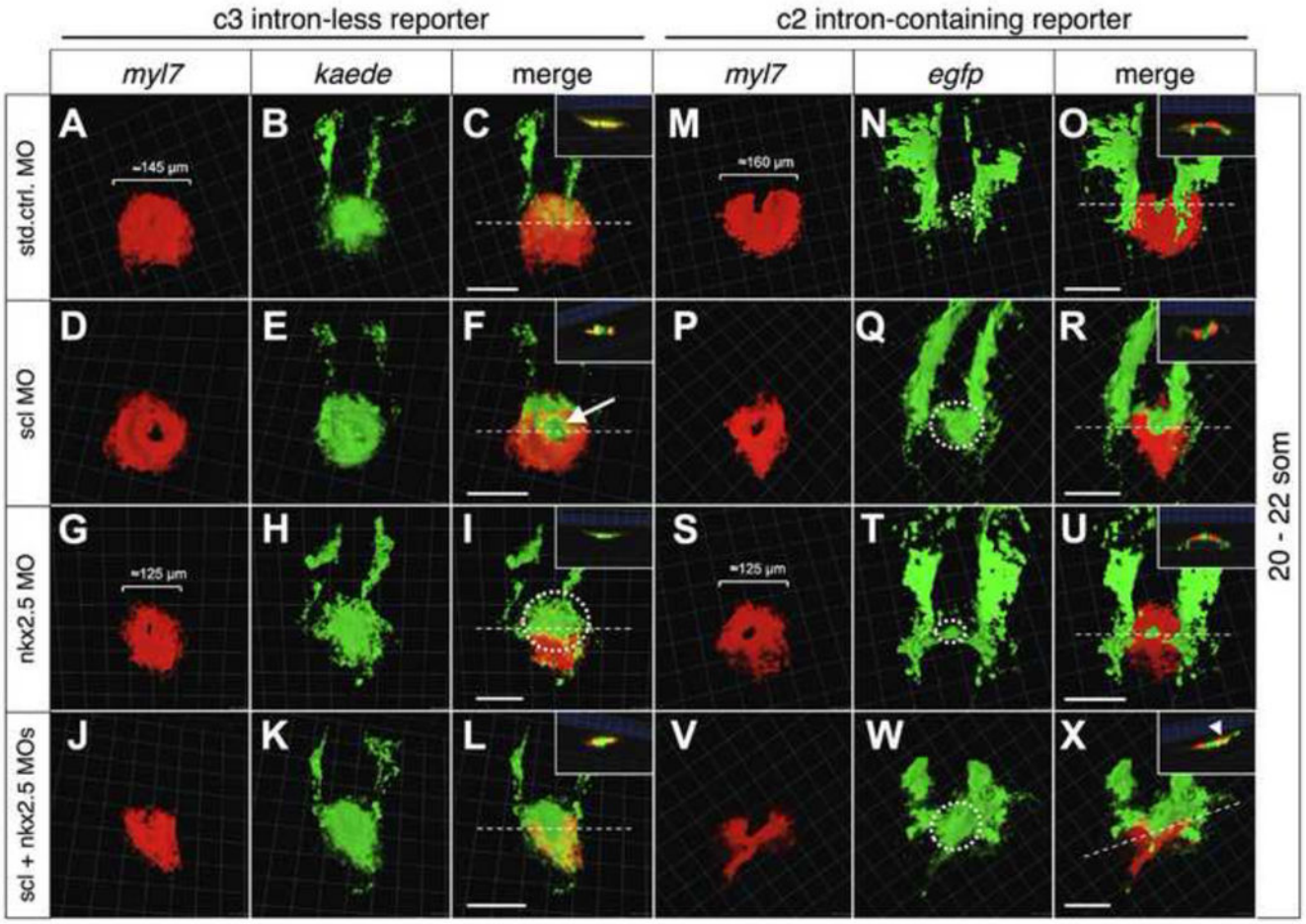

Figure 4. Spatial changes in intron-less c3 and intron-containing c2 transgene expression in *scl / nkx2.5* morphant cardiac discs

Display of *myl7*+ myocardial progenitor cells (red) and concomitant display of cells expressing either c3 *kaede*+ (**A-L**) or c2 *egfp*+ (**M-X**) reporter transgenes (green) by two-color fluorescent in-situ-hybridization. Merged images are shown in (**C, F, I, L**) and (**O, R, U, X**), respectively, with insets showing transverse optical sections at the section plane indicated by dashed lines. In control embryos, the c3 transgene expression shows maximal overlap with the flat and disc-shape myocardial *myl7*+ expression domain (**A-C**, similar as in Figure S2M-O), but the c2 transgene expression marking the endocardial domain (dashed circle in **N**) shows minimal overlap (**M-O**). In *scl* morphants, the endocardial domains of both c3 (**D-F**) and *c2* (**P-R**) transgenes were enlarged (indicated by arrow in F and dashed circle in **Q**), resulting in compaction of the myocardial domain around the enlarged endocardial domain (see insets). In *nkx2.5* morphants, the size of the myocardial disc was reduced (compare **G** and **S** to **A** and **M**), however the myocardial c3 transgene expression domain (**G-I**) was increased (dashed circle in **I**). The size of the endocardial domain marked by the c2 transgene was unchanged in *nkx2.5* morphant cardiac discs (**S-U**, dashed circle in **T**). In double *scl/nkx2.5* knockdown embryos, cardiac expression of the intron-less c3 transgene was increased in both endocardial and myocardial domains (**J-L**), and intron-less c2 transgene expression showed an increase in the endocardial domain (**V-X**). Note *myl7*+

c2 transgene expressing cells in *scl/nkx2.5* double morphants indicated by arrowhead in the transverse optical section in inset of **X**). Approximate myocardial domain sizes are given in **A, M, G** and **S**. Embryos are 20-22 som in dorsal views with anterior to the top from one c3 line (F5 generation) and one c2 line (F4). Images shown are snapshots from 3D views with bars ≈100 μm in relation to the background grid (1 unit = 45.18 μm). Transverse optical sections (insets) were scaled down 0.6x.

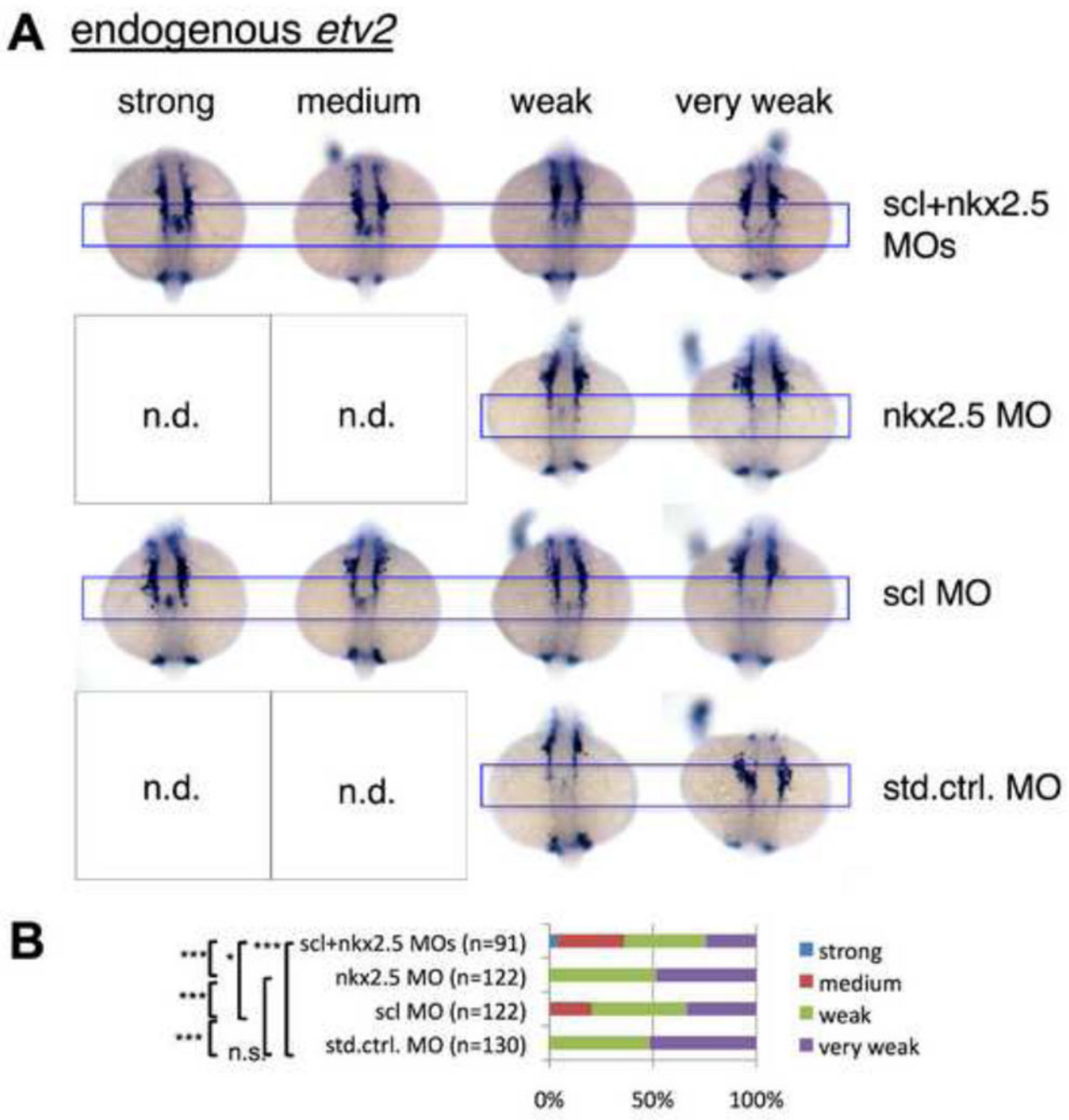

Figure 5. Response of endogenous *etv2* expression to single and combined knockdowns of *nkx2.5* and *scl* in the cardiac disc

(A) Representative embryos showing categories of *etv2* expression in the endocardial domain of the cardiac disc following single and combined knockdowns of *scl* and *nkx2.5* and quantification in **(B)**. Note that single *nkx2.5* morpholino knockdown resulted in no significant modulation of *etv2* expression but further increased the effect of *scl* morpholino in double knockdown experiments. Embryos shown are at 20-22 som stages in dorsal view with anterior to the top. *** indicates p≤0.001; ** indicates p≤0.01; * indicates p≤0.05,

n.s.=not significant ($p>0.05$); n.d.=not detected; MO=morpholino; n=number of scored embryos; blue frame marks the endocardial cardiac disc expression domain of *etv2*. Categories of transgene expression magnitudes scored are color-coded in **(B)**.

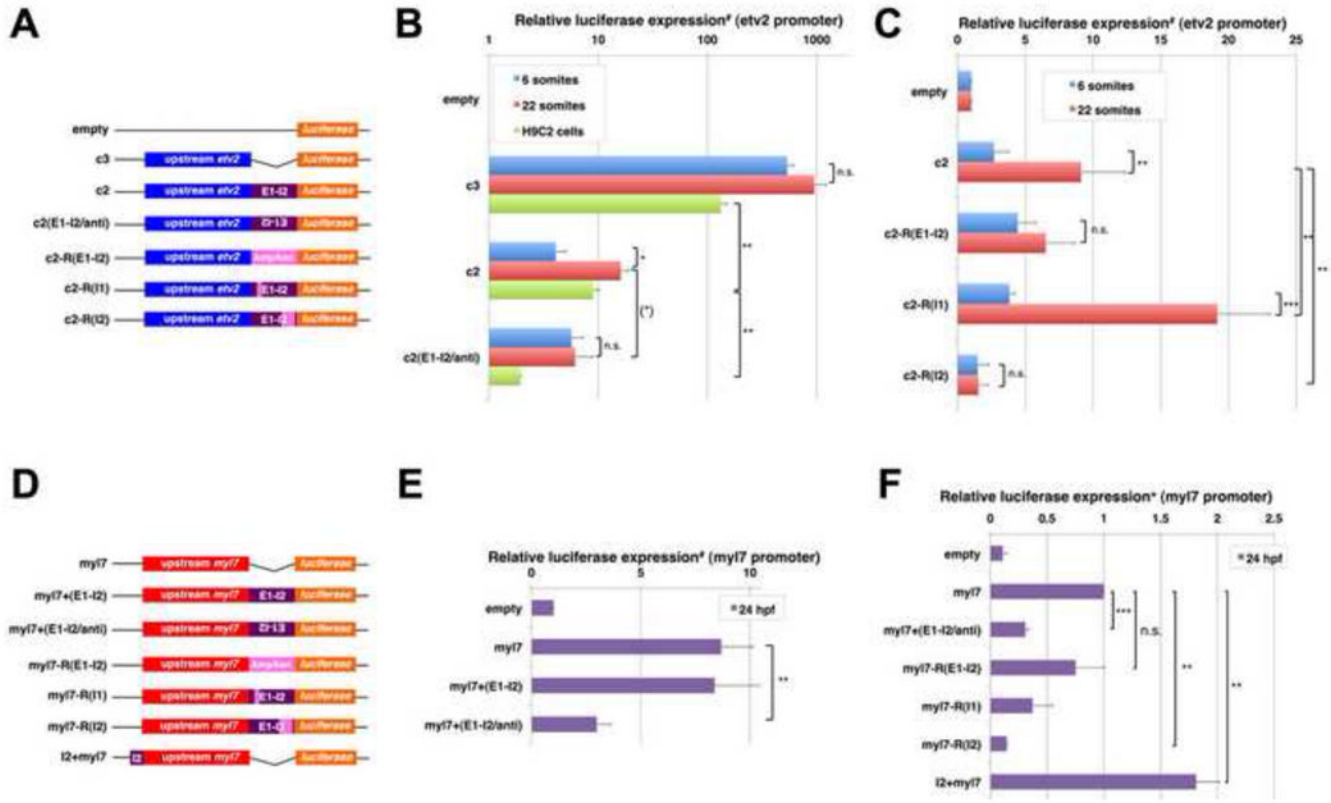

Figure 6. *etv2* and *myl7* promoter activity using dual-luciferase reporter assays in zebrafish embryos and cardiac cell line

(**A**) Cartoon of etv2 promoter constructs designed for dual-luciferase reporter assays in embryos and cell line is depicted. Anti: antiparallel, E: exon, I: intron, R: replacement. (**B**) Relative luciferase expression for constructs c2, c3 and c2(E1-I2/anti) in 6 and 22 somite embryos and H9C2 cardiac cell line is shown. (**C**) Relative luciferase expression for etv2 constructs c2, c2-R(E1-I2), c2-R(I1) and c2-R(I2) in 6 and 22 somite embryos is shown. **(D)** Cartoon of myl7 promoter constructs designed for dual-luciferase reporter assays in embryos and cell line is depicted. Anti: antiparallel, E: exon, I: intron, R: replacement. (**E**) Relative luciferase expression for myl7 constructs myl7, myl7 plus etv2 downstream sequence (E1-I2), and myl7 plus etv2 downstream sequence in antiparallel orientation (E1-I2/anti) in 24 hpf embryos is shown. (**F**) Relative luciferase expression for myl7 constructs myl7, myl7 plus etv2 downstream sequence in antiparallel orientation (E1-I2/anti), myl7 plus ampicillin/kanamycin sequence [R(E1-I2)], myl7 plus etv2 downstream sequence with intron 1 replacement [R(I1)], myl7 plus etv2 downstream sequence with intron 2 replacement [R(I2)], and etv2 intron 2 placed upstream of the myl7 promoter (I2+myl7) in 24 hpf embryos is shown.For panels B, C, E and F, statistical analysis using *t* test was performed across sample groups. Error bars indicate standard deviations. #: expression relative to empty vector, +: expression relative to myl7 promoter. *** denote P≤0.001** denote P≤0.01; * denotes P≤0.05, n.s.=not significant (P>0.05).

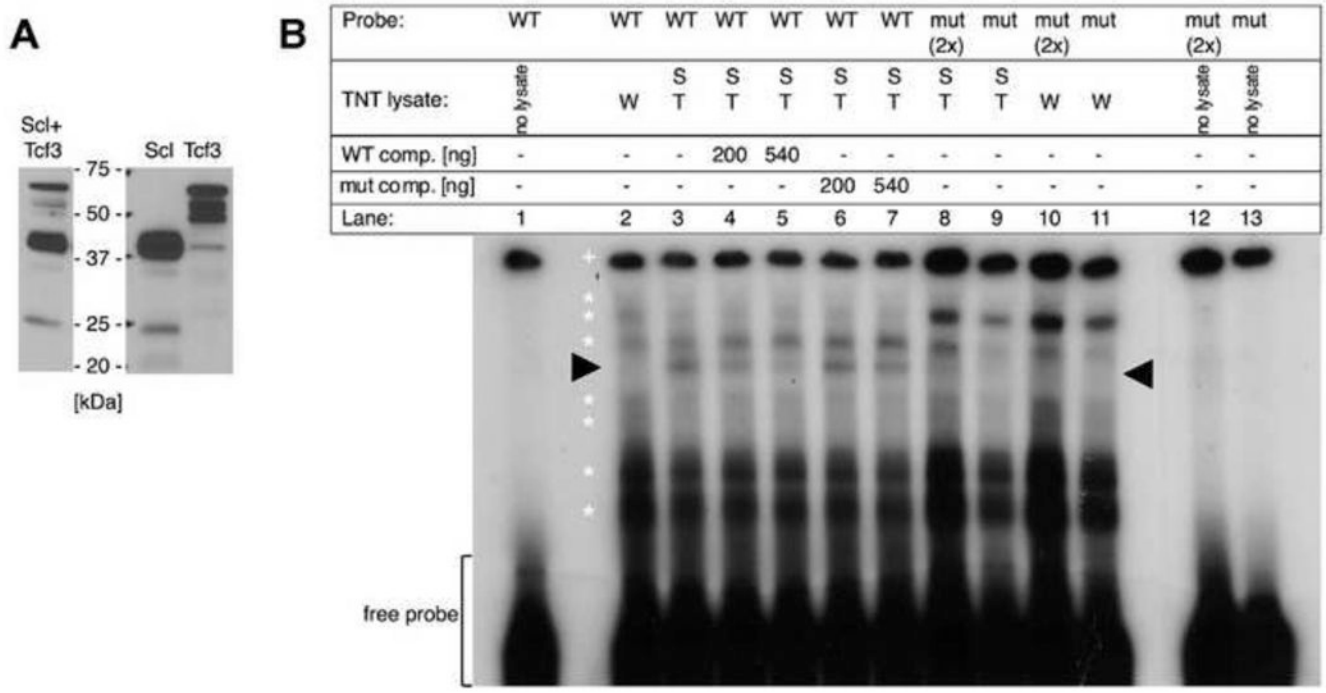

Figure 7. Recombinant Scl protein bound to an E-box motif in the *etv2* proximal promoter

(**A**) Detection of in-vitro-translated FLAG-tagged Scl and Tcf3 proteins by western blot. Co-expressed (left) and single-expressed (right) proteins are shown. (**B**) Lysates that contained coexpressed proteins (ST; lanes 3-9) or unprocessed lysates (W; lanes 2, 10, 11) were incubated with radiolabelled probes harboring either the wildtype (WT; lanes 1-7) or mutated (mut; lanes 8-13) E-box motif in the presence of increasing amounts of either wildtype or mutated competitor DNA (WT comp., lanes 4 & 5; mut comp., lanes 6 & 7; 200 and 540 ng, respectively). After non-denaturing gel electrophoresis and autoradiography, an E-box motif-specific complex (position indicated by black arrowhead) was detected when ST lysate was used (lanes 3-7) and disappeared when WT competitors were present (lanes 4 &5). Mutated competitor DNA had only minimal effect on complex formation (lanes 6 & 7). This complex was not detected using mutated probes (lanes 8-11). Free probes were displayed without lysates (lanes 1, 12 & 13). White stars indicate non-specific complexes.